THE JOURNAL OF BIOLOGICAL CHEMISTRY
Vol. 280, No. 27, Issue of July 8, pp. 25313–25322, 2005

Printed in U.S.A.

O-GlcNAcase Uses Substrate-assisted Catalysis

KINETIC ANALYSIS AND DEVELOPMENT OF HIGHLY SELECTIVE MECHANISM-INSPIRED INHIBITORS*[S]

Received for publication, December 8, 2004, and in revised form, March 3, 2005
Published, JBC Papers in Press, March 28, 2005, DOI 10.1074/jbc.M413819200

Matthew S. Macauley, Garrett E. Whitworth, Aleksandra W. Debowski, Danielle Chin, and David J. Vocadlo‡

From the Department of Chemistry, Simon Fraser University, Burnaby, British Columbia V5A 1S6, Canada

The post-translational modification of serine and threonine residues of nucleocytoplasmic proteins with 2-acetamido-2-deoxy-D-glucopyranose (GlcNAc) is a reversible process implicated in multiple cellular processes. The enzyme *O*-GlcNAcase catalyzes the cleavage of β-*O*-linked GlcNAc (*O*-GlcNAc) from modified proteins and is a member of the family 84 glycoside hydrolases. The family 20 β-hexosaminidases bear no apparent sequence similarity yet are functionally related to *O*-GlcNAcase because both enzymes cleave terminal GlcNAc residues from glycoconjugates. Lysosomal β-hexosaminidase is known to use substrate-assisted catalysis involving the 2-acetamido group of the substrate; however, the catalytic mechanism of human *O*-GlcNAcase is unknown. By using a series of 4-methylumbelliferyl 2-deoxy-2-*N*-fluoroacetyl-β-D-glucopyranoside substrates, Taft-like linear free energy analyses of these enzymes indicates that *O*-GlcNAcase uses a catalytic mechanism involving anchimeric assistance. Consistent with this proposal, 1,2-dideoxy-2′-methyl-α-D-glucopyranoso-[2,1-*d*]-Δ2′-thiazoline, an inhibitor that mimics the oxazoline intermediate proposed in the catalytic mechanism of family 20 glycoside hydrolases, is shown to act as a potent competitive inhibitor of both *O*-GlcNAcase (K_I = 0.070 μM) and β-hexosaminidase (K_I = 0.070 μM). A series of 1,2-dideoxy-2′-methyl-α-D-glucopyranoso-[2,1-*d*]-Δ2′-thiazoline analogues were prepared, and one inhibitor demonstrated a remarkable 1500-fold selectivity for *O*-GlcNAcase (K_I = 0.230 μM) over β-hexosaminidase (K_I = 340 μM). These inhibitors are cell permeable and modulate the activity of *O*-GlcNAcase in tissue culture. Because both enzymes have vital roles in organismal health, these potent and selective inhibitors of *O*-GlcNAcase should prove useful in studying the role of this enzyme at the organismal level without generating a complex chemical phenotype stemming from concomitant inhibition of β-hexosaminidase.

Humans have three genes encoding enzymes that cleave terminal *N*-acetylglucosamine residues from glycoconjugates. The first of these, *O*-GlcNAcase,[1] is a member of family 84 of glycoside hydrolases that includes enzymes from organisms as diverse as prokaryotic pathogens and humans (1, 2).[2] The substrates of *O*-GlcNAcase are post-translationally modified glycoproteins bearing the monosaccharide 2-acetamido-2-deoxy-β-D-glucopyranoside linked to serine or threonine residues (*O*-GlcNAc) (3–5). This post-translational modification is abundant in mammalian cells (3) and is found on many cellular proteins having a wide range of vital cellular functions, including for example, transcription (6–9), proteasomal degradation (10), and cellular signaling (11), and is also found on many structural proteins (12–14). Consistent with the abundance of *O*-GlcNAc on intracellular proteins, it appears to have roles in the etiology of several disease states, including type II diabetes (11, 15), Alzheimer (13, 16, 17), and cancer (18). Although *O*-GlcNAcase was likely isolated earlier on (19, 20), an understanding of its biochemical role in acting to cleave *O*-GlcNAc off from modified serine and threonine residues of proteins waited some 20 years (21). More recently *O*-GlcNAcase has been cloned (23), partially characterized (24), and suggested to have additional activity as a histone acetyltransferase (22). Little, however, is known about the catalytic mechanism of this enzyme.

HEXA and *HEXB* are the two other genes that encode enzymes catalyzing the hydrolytic cleavage of terminal *N*-acetylglucosamine residues from glycoconjugates. The gene products of *HEXA* and *HEXB* predominantly yield two dimeric isozymes. The homodimeric isozyme, hexosaminidase B (ββ), is composed of two β-subunits, and the heterodimeric isozyme, hexosaminidase A (αβ), is composed of an α- and a β-subunit. Both of these enzymes are normally localized within the lysosome. The two subunits bear a high level of sequence identity, and both are members of family 20 of glycoside hydrolases. The dysfunction of either of these isozymes results in the accumulation of gangliosides and other glycoconjugates within the lysosome causing the inheritable neurodegenerative disorders known as Tay-Sachs and Sandhoff diseases (25). The deleterious effects of accumulation of gangliosides at the organismal level are still being uncovered (26). In contrast, the consequences of genetic deletion of *O*-GlcNAcase remain unknown.

Small molecule inhibitors of glycosidases, including β-*N*-acetyl-glucosaminidases (27–30), have received a great deal of

* This work was supported by grants from the Natural Sciences and Engineering Research Council of Canada, the Protein Engineering Networks of Centres of Excellence Research Chairs Program, starting funds from Simon Fraser University, and a President's Research Grant. The costs of publication of this article were defrayed in part by the payment of page charges. This article must therefore be hereby marked "*advertisement*" in accordance with 18 U.S.C. Section 1734 solely to indicate this fact.

[S] The on-line version of this article (available at http://www.jbc.org) contains supplemental Figs. 1 and 2.

‡ Recipient of a Tier II Research Chair from the Canada Research Chairs Program. To whom correspondence should be addressed: Dept. of Chemistry, Simon Fraser University, 8888 University Blvd., Burnaby, British Columbia V5A 1S6, Canada. E-mail: dvocadlo@sfu.ca.

[1] The abbreviations used are: *O*-GlcNAcase, *O*-glycoprotein 2-acetamido-2-deoxy-β-D-glucopyranosidase; GlcNAc, 2-acetamido-2-deoxy-D-glucopyranose; Py, pyridine; 4-MU, 4-methylumbelliferone; *p*NP-GlcNAc, *para*-nitrophenyl-GlcNAc; STZ, streptozotocin; PUGNAc, *O*-(2-acetamido-2-deoxy-D-glucopyranosylidene)amino-*N*-phenylcarbamate; NAG-thiazoline, 1,2-dideoxy-2′-methyl-α-D-glucopyranoso-[2,1-*d*]-Δ2′-thiazoline; DCC, dicyclohexylcarbodiimide; DMF, dimethylformamide; PBS, phosphate-buffered saline; HRP, horseradish peroxidase; mAb, monoclonal antibody; BSA, bovine serum albumin.

[2] For the family classification of glycoside hydrolases, see Refs. 1 and 2 and the CAZY Database (available at afmb.cnrs-mrs.fr/CAZY/).

attention (31) both as tools for elucidating the role of these enzymes in biological processes as well as in developing therapeutic interventions with minimal side effects. Indeed, the control of glycosidase function using small molecules offers several advantages over genetic knock-out studies, including the ability to rapidly vary dose or entirely withdraw treatment. A major hurdle, however, in the generation of selective inhibitors of human glycosidases is that multiple functionally related enzymes are often present within a given organism. The promiscuity of many inhibitors and the resultant inhibition of multiple enzymes render them of limited utility in studying the cellular and organismal physiological role of one particular enzyme because they necessarily generate complex phenotypes. In the case of β-*N*-acetylglucosaminidase no potent inhibitor is currently known that is selective for nucleocytoplasmic *O*-GlcNAcase over the lysosomal β-hexosaminidases.

Two existing inhibitors of *O*-GlcNAcase, however, have enjoyed use in studies of the *O*-GlcNAc post-translational modification within both cells and tissues (11, 32–35). Both of these compounds, however, suffer from having secondary effects within the cellular and organismal environment. Streptozotocin (STZ) has long been used as a diabetogenic compound because it has a particularly detrimental effect on β-islet cells (36). STZ exerts its cytotoxic effects through both the alkylation of cellular DNA (36, 37) as well as the generation of radical species, including nitric oxide (38). The resulting DNA strand breakage promotes the activation of poly(ADP-ribose) polymerase (39) with the net effect of depleting cellular NAD^+ levels and, ultimately, leading to cell death (40, 41). Other investigators have proposed instead that STZ toxicity is a consequence of the irreversible inhibition of *O*-GlcNAcase, which is highly expressed within islet β-cells (32, 42). This hypothesis has, however, been brought into question by two independent research groups (43, 44). Because cellular *O*-GlcNAc levels increase in response to many forms of cellular stress (45), it seems possible that STZ results in increased *O*-GlcNAc levels by inducing cellular stress rather than through any specific and direct action on *O*-GlcNAcase. Indeed, Hanover *et al.* (46) have shown that STZ functions as a poor and somewhat selective inhibitor of *O*-GlcNAcase, and although it has been proposed by others that STZ acts to irreversibly inhibit *O*-GlcNAcase (47), there has been no clear demonstration of this mode of action.

The second compound that has enjoyed use as an inhibitor of *O*-GlcNAcase is *O*-(2-acetamido-2-deoxy-D-glucopyranosylidene)amino-*N*-phenylcarbamate (PUGNAc). Rast and co-workers (28) described the potent inhibitory properties of PUGNAc on β-*N*-acetylglucosaminidases from *Canavalia ensiformis*, *Mucor rouxii,* and the family 20 β-hexosaminidase from bovine kidney. This compound has also been shown to be a highly potent inhibitor of mouse β-hexosaminidase (48). More recent studies have demonstrated that PUGNAc is also a potent inhibitor of the family 84 *O*-GlcNAcase (21) that lacks the cytotoxic effects of STZ (49). Despite its apparent lack of short term toxicity, this compound is a potent inhibitor of both the family 20 and family 84 glycoside hydrolases, and therefore *in vivo* studies using this compound will yield a complex phenotype stemming from the inhibition of these functionally related enzymes.

Given these considerations, we felt that the development of a potent, cell-permeable inhibitor selective for *O*-GlcNAcase over the lysosomal β-hexosaminidases would be a valuable tool in studying the physiological role of *O*-GlcNAc at the cellular and organismal level. A logical starting point for the design of such an inhibitor for *O*-GlcNAcase would take into consideration the catalytic mechanism of these two functionally related enzymes. Although the catalytic mechanisms of action of the family 20 human β-hexosaminidases A and B have been fairly well established (50), that of the family 84 *O*-GlcNAcase remains unknown. We therefore aimed to first elucidate the catalytic mechanism of human *O*-GlcNAcase and second to use this information in designing simple inhibitors that would be potent, cell permeable, and highly selective for *O*-GlcNAcase over the lysosomal β-hexosaminidases.

EXPERIMENTAL PROCEDURES

General Procedures for Synthesis of Compounds—All buffer salts used in this study were obtained from Sigma. Dry methanol and toluene were purchased from Acros Organics. Dicloromethane and triethylamine were dried by distillation over CaH_2 prior to use. β-Hexosaminidase was purchased from Sigma (lot 043K3783). STZ was purchased from Sigma, and samples were freshly dissolved just prior to assays. PUGNAc was obtained from Toronto Research Chemicals. All other reagents were purchased from Sigma and used without further purification. Milli-Q (18.2 megohms cm^{-1}) water was used to prepare all buffers. Synthetic reactions were monitored by TLC using Merck Kieselgel 60 F_{254} aluminium-backed sheets. Compounds were detected by charring with 10% ammonium molybdate in 2 M H_2SO_4 and heating. Flash chromatography under a positive pressure was performed with Merck Kieselgel 60 (230–400 mesh) using the specified eluants. ^1H NMR spectra were recorded on a Varian AS500 Unity Innova spectrometer at 500 MHz (chemical shifts quoted relative to $CDCl_3$, CD_3OD, or $(CD_3)_2SO$ where appropriate). ^{19}F NMR spectra were recorded on a Varian AS500 Unity Innova spectrometer at 470 MHz and are proton-coupled with CF_3CO_2H as a reference. ^{13}C NMR spectra were recorded on a Varian AS500 Unity Innova spectrometer at 125 MHz (chemical shifts quoted relative to $CDCl_3$, CD_3OD, or $(CD_3)_2SO$). Elemental analyses of all compounds used in cell culture and enzyme assay were performed at the Simon Fraser University Analytical Facility.

Synthesis of 4-Methylumbelliferone 2-Deoxy-2-acetamido-β-D-glucopyranosides—4-Methylumbelliferyl 2-amino-2-deoxy-β-D-glucopyranoside hydrochloride (**3**) was prepared essentially as described by Roeser and Legler (51) and was used without further purification.

4-Methylumbelliferyl 3,4,6-Tri-O-acetyl-2-deoxy-2-trifluoroacetamido-β-D-glucopyranoside—Triethylamine (0.06 ml, 0.042 g, 0.41 mmol) was added to a cooled (0 °C) solution of the hydrochloride salt **3** (0.10 g, 0.2 mmol) in a solution of dimethylformamide (DMF, 6 ml). The reaction mixture was then cooled to 0 °C, and trifluoroacetic anhydride (0.08 ml, 0.12 g, 5.7 mmol) was added via syringe. The resulting solution was allowed to stand for 16 h at 0 °C, after which time the reaction was judged complete by TLC analysis. The reaction mixture was then diluted with ethyl acetate (20 ml), and a solution of saturated sodium chloride (40 ml) was added. The organic layer was collected, and the aqueous layer was extracted twice with ethyl acetate. The combined organic extracts were washed successively with water, twice with saturated sodium bicarbonate, and finally with a solution of saturated sodium chloride. The organic extracts were dried over $MgSO_4$ and filtered, and the solvent was removed *in vacuo* to yield a light yellow syrup. The desired product was purified using flash column silica chromatography using a gradient solvent system (1:1; hexanes/ethyl acetate) to yield the partially purified desired compound as an amorphous white solid (≈0.093 g, 0.17 mmol, 82%) that was used in the next step without further purification.

4-Methylumbelliferyl 3,4,6-Tri-O-acetyl-2-deoxy-2-difluoroacetamido-β-D-glucopyranoside—Triethylamine (0.09 ml, 0.063 g, 0.62 mmol) and dry pyridine (3 ml) were added to a cooled (0 °C) solution of the hydrochloride salt **3** (0.15 g, 0.3 mmol) in a solution of DMF (6 ml). Dicyclohexylcarbodiimide (DCC, 0.48 g, 2.3 mmol) and difluoroacetic acid (0.12 ml, 0.18 g, 1.3 mmol) were added to the reaction mixture via syringe. The resulting solution was allowed to stand for 16 h at 0 °C, after which time 2 drops of difluoroacetic acid were added. After a further 3.5 h at room temperature, the reaction was judged complete by TLC analysis. The solvent was partially removed *in vacuo*, and then ethyl acetate (50 ml) and a solution of saturated sodium chloride (20 ml) were added. The organic layer was collected, and the aqueous layer was extracted twice with ethyl acetate. The combined organic extracts were washed successively with water, twice with saturated sodium bicarbonate, and finally with a solution of saturated sodium chloride. The organic extracts were dried over $MgSO_4$ and filtered, and the solvent was removed *in vacuo* to yield a light yellow syrup. The desired product was purified using flash column silica chromatography using a gradient solvent system (1:1; hexanes/ethyl acetate) to yield the partially purified desired compound as a white amorphous solid (≈0.10 g, 0.19 mmol, 64%) that was used in the next step without further purification.

4-Methylumbelliferyl 3,4,6-Tri-O-acetyl-2-deoxy-2-fluoroacetamido-β-D-glucopyranoside—Triethylamine (0.3 ml, 0.21 g, 2.1 mmol) and dry pyridine (10 ml) were added to a cooled (0 °C) solution of the hydrochloride salt **3** (0.50 g, 1.0 mmol) in a solution of DMF (10 ml). Sodium fluoroacetate (0.9 g) was added to a stirred mixture of dry DMF (45 ml) containing dried Dowex 50-H^+ resin (6 g). (*Caution*: fluoroacetic acid is highly toxic, and proper precautions must be taken during its use and disposal!) After 1 h, DCC (1.6 g, 7.8 mmol) and 30 ml of the fluoroacetic acid solution (6.0 mmol) were added via cannula to the reaction vessel containing the hydrochloride salt **3**. The resulting solution was allowed to stand for 16 h at 0 °C, after which time the reaction was judged complete by TLC analysis. The solvent was partially removed *in vacuo*, after which ethyl acetate (50 ml) and a solution of saturated sodium chloride (20 ml) were added. The organic layer was collected, and the aqueous layer was extracted twice with ethyl acetate. The combined organic extracts were washed successively with water, twice with saturated sodium bicarbonate, and finally with a solution of saturated sodium chloride. The organic extracts were dried over $MgSO_4$ and filtered, and the solvent was removed *in vacuo* to yield a light yellow syrup. The desired product was purified using flash column silica chromatography (2:1; ethyl acetate/hexanes) to yield the partially purified desired compound as an amorphous white solid (≈0.36 g, 0.68 mmol, 68%) that was used in the next step without further purification.

General Procedure for the Synthesis of 4-Methylumbelliferyl 2-Deoxy-2-fluoroacetamido-β-D-glucopyranosides—A spatula tip of anhydrous sodium methoxide was added to a solution of each glycoside in dry methanol. The resulting basic solution was stirred under nitrogen until the reaction was judged complete by TLC analysis. Dowex 50-H^+ resin was added to the stirred reaction mixture until the pH of the solution became neutral. The suspension was filtered, and the filter cake was rinsed extensively with methanol, after which the solvent from the combined filtrates was removed *in vacuo*. The desired deprotected glycosides were isolated by flash column silica chromatography using the following solvent systems: ethyl acetate/methanol/water (12:1:1) for the *N*-tri- and *N*-difluoroacetyl derivatives (**5b** and **5c**) and ethyl acetate/methanol (1:1) for the *N*-monofluoroacetyl derivative (**5a**). Products were recrystallized from ethanol and diethyl ether to yield the desired products with the overall yields over two steps of 66% for the *N*-trifluoroacetyl derivative (**5c**), 37% for the *N*-difluoroacetyl derivative (**5b**), and 45% for the *N*-fluoroacetyl derivative (**5a**).

*4-Methylumbelliferyl 2-Deoxy-2-fluoroacetamido-β-D-glucopyranoside (**5a**)*—^{1}H NMR (500 MHz, d_6-Me_2SO) δ 7.71 (1H, d, $J_{H5AR\text{-}H6AR}$ = 8.8, H-5_{AR}), 7.00 (1H, $J_{H8AR\text{-}H6AR}$ = 2.4, H-8_{AR}), 6.96 (1H, dd, H-6_{AR}), 6.26 (1H, d, $J_{H3AR\text{-}CH3}$ = 1.1, H-3_{AR}), 5.21 (1H, d, $J_{H1\text{-}H2}$ = 8.5, H-1), 4.81 (2H, d, $J_{H\text{-}F}$ = 47.0, CH_2F), 3.86 (1H, dd, $J_{H2\text{-}H3}$ = 9.9, H-2), 3.74 (1H, dd, $J_{H6\text{-}H6'}$ = 11.7, $J_{H6\text{-}H5}$ = 1.7, H-6), 3.53–3.46 (2H, m, H-3, H-6′), 3.38 (1H, ddd, $J_{H5\text{-}H4}$ = 9.6, $J_{H5\text{-}H6'}$ = 6.0, H-5), 3.20 (1H, dd, $J_{H4\text{-}H3}$ = 8.9, H-4), 2.39 (1H, d, CH_3) ppm; ^{19}F NMR (500 MHz, d_6-Me_2SO) −225.24 (dd, $J_{F\text{-}H}$ = 53) ppp;

$C_{18}\ H_{20}\ FNO_8$

Calculated:	C 54.41	H 5.07	N 3.53
Found:	C 54.20	H 4.97	N 3.59

*4-Methylumbelliferyl 2-Deoxy-2-difluoroacetamido-β-D-glucopyranoside (**5b**)*—^{1}H NMR (500 MHz, d_6-Me_2SO) δ 7.69 (1H, d, $J_{H5AR\text{-}H6AR}$ = 8.8, H-5_{AR}), 6.97 (1H, $J_{H8AR\text{-}H6AR}$ = 2.4, H-8_{AR}), 6.92 (1H, dd, H-6_{AR}), 6.24 (1H, d, $J_{H3AR\text{-}CH3}$ = 1.2, H-3_{AR}), 6.21 (1H, d, $J_{H\text{-}F}$ = 53.6 Hz, CHF_2), 5.16 (1H, d, $J_{H1\text{-}H2}$ = 8.5, H-1), 3.79 (1H, dd, $J_{H2\text{-}H3}$ = 10.3, H-2), 3.72 (1H, dd, $J_{H6\text{-}H6'}$ = 11.8, $J_{H6\text{-}H5}$ = 1.9, H-6), 3.53–3.42 (2H, m, H-3, H-5, H-6′), 3.20 (1H, dd, $J_{H4\text{-}H5}$ = 9.6 Hz, $J_{H4\text{-}H3}$ = 8.9 Hz, H-4), 2.38 (1H, d, CH_3) ppm; ^{19}F NMR (500 MHz, d_6-Me_2SO) −127.32 (d, J = 54 Hz);

$C_{18}\ H_{19}F_2\ NO_8$

Calculated:	C 52.05	H 4.61	N 3.37
Found:	C 51.92	H 4.62	N 3.31

*4-Methylumbelliferyl 2-Deoxy-2-Trifluoroacetamido-β-D-glucopyranoside (**5c**)*—^{1}H NMR (500 MHz, d_6-Me_2SO) δ 7.70 (1H, d, $J_{H5AR\text{-}H6AR}$ = 8.8, H-5_{AR}), 6.86 (1H, $J_{H8AR\text{-}H6AR}$ = 2.3, H-8_{AR}), 6.91 (1H, dd, H-6_{AR}), 6.25 (1H, d, $J_{H3AR\text{-}CH3}$ = 1.2, H-3_{AR}), 5.16 (1H, d, $J_{H1\text{-}H2}$ = 8.5, H-1), 3.80 (1H, dd, $J_{H2\text{-}H3}$ = 10.2, H-2), 3.72 (1-H, dd, $J_{H6\text{-}H6'}$ = 11.7, $J_{H6\text{-}H5}$ = 1.8, H-6), 3.50–3.42 (2H, m, H-6′, H-3, H-5), 3.22 (1H, dd, $J_{H4\text{-}H5}$ = 9.5 Hz, $J_{H4\text{-}H3}$ = 8.9 Hz, H-4), 2.38 (1H, d, CH_3) ppm; ^{19}F NMR (500 MHz, d_6-Me_2SO) −77.29;

$C_{18}\ H_{18}\ F_3NO_8$

Calculated:	C 49.89	H 4.19	N 3.23
Found:	C 49.80	H 4.29	N 3.11

Kinetic Analysis of O-GlcNAcase and β-Hexosaminidase—All assays were carried out in triplicate at 37 °C for 30 min by using a stopped assay procedure in which the enzymatic reactions (25 μl) were quenched by the addition of a 6-fold excess (150 μl) of quenching buffer (200 mM glycine, pH 10.75). Assays were initiated by the addition, via syringe, of enzyme (3 μl), and in all cases the final pH of the resulting quenched solution was greater than 10. Time-dependent assay of β-hexosaminidase and *O*-GlcNAcase revealed that both enzymes were stable over this period in their respective buffers: 50 mM citrate, 100 mM NaCl, 0.1% BSA, pH 4.25, and 50 mM NaH_2PO_4, 100 mM NaCl, 0.1% BSA, pH 6.5. The progress of the reaction at the end of 30 min was determined by measuring the extent of 4-methylumbelliferone liberated as determined by fluorescence measurements using a Varian CARY Eclipse Fluorescence Spectrophotometer 96-well plate system and comparison to a standard curve of 4-methylumbelliferone under identical buffer conditions. Excitation and emission wavelengths of 368 and 450 nM were used, respectively, with 5 mm slit openings. The possible time-dependent inactivation of *O*-GlcNAcase was assayed by incubating 10 mM STZ with 0.016 mg/ml *O*-GlcNAcase in the presence of 50 mM NaH_2PO_4, 100 mM NaCl, 1% BSA, 5 mM β-mercaptoethanol, pH 6.5, or 0.036 mg/ml β-hexosaminidase in the presence of 50 mM citrate, 100 mM NaCl, 0.1% BSA, pH 4.25. At several time intervals, the residual enzyme activity contained in the inactivation mixture was assayed. Assays were carried out as described above for each enzyme except that reactions were initiated by the addition of an aliquot of the reaction mixture into the assay mixture containing 5.7 mM MU-GlcNAc and the appropriate buffer for each enzyme. The stability of STZ was first tested by following its decomposition in deuterated water by NMR. The half-life of STZ in aqueous solution at room temperature was greater than 6 h as determined by following its decomposition by NMR at room temperature. Human placental β-hexosaminidase was purchased from Sigma (lot 043K3783). The cloning and expression of *O*-GlcNAcase will be described elsewhere. Both enzymes were dialyzed against PBS buffer and their concentrations determined with the Bradford assay using BSA as a standard. The concentrations (μg/μl) of β-hexosaminidase and *O*-GlcNAcase used in assays with fluorinated substrates were as follows: for 4-methylumbelliferyl 2-acetamido-2-deoxy-β-D-glucopyranoside (**5**), 0.00077, 0.0126; **5a**, 0.0031, 0.0189; **5b**, 0.0154, 0.0756; and for **5c**, 0.0154, 0.01523. In addition, β-hexosaminidase and *O*-GlcNAcase were used in inhibition assays at a concentration (μg/μl) of 0.0154 and 0.0378, respectively, using substrate **5** at a concentration of 0.64 mM. All inhibitors were tested at eight concentrations ranging from 5 times to 1/5th K_I, with the exception of the assay of inhibitor **8e** with β-hexosaminidase, where a such high concentrations of inhibitor could not be reached because of the high K_I value of **8e**. K_I values were determined by linear regression of data from Dixon plots. Where necessary, assays were carried out in triplicate, and error bars are included in plots of the data.

General Procedure for the Synthesis of 1,3,4,6-Tetra-O-acetyl-2-deoxy-2-N-acyl-β-D-glucopyranoses—Two eq of dry triethylamine was added to a solution of the hydrochloride salt of 2-amino-2-deoxy-1,3,4,6-tetra-*O*-acetyl-β-D-glucopyranose (**6**) (52) in 1 volume of dry dichloromethane, at which time the starting material dissolved. The reaction mixture was cooled to 0 °C, and 1.2 eq of the appropriate acyl chloride was added via syringe. The resultant mixture was stirred for approximately 2 h at room temperature. When the reaction mixture was judged complete by TLC analysis, 5 volumes of ethyl acetate were added. The resulting organic phase was washed successively with water, 1 M NaOH, and saturated sodium chloride. The organic phase was dried over $MgSO_4$, filtered, and concentrated to yield a white crystalline solid. The material was recrystallized using a mixture of ethyl acetate and hexanes to yield the desired *N*-acylated materials in yields ranging from 46 to 74%.

*1,3,4,6-Tetra-O-acetyl-2-deoxy-2-N-propyl-β-D-glucopyranose (**7b**)*—^{1}H NMR (500 MHz, $CDCl_3$) δ: 5.68 (1H, d, $J_{H1,H2}$ = 8.8 Hz, H-1), 5.42 (1H, d, $J_{NH,H2}$ = 6.7 Hz, NH), 5.14 (1H, dd, $J_{H3,H4}$ = 8.7 Hz, H-3), 5.12 (1H, dd, $J_{H4,H5}$ = 8.7 Hz, H-4), 4.34 (1H, ddd, $J_{H2,H3}$ = 8.7 Hz, H-2), 4.27 (1H, dd, $J_{H6,H6'}$ = 12.5 Hz, $J_{H5,H6}$ = 4.6 Hz, H-6), 4.12 (1H, dd, $J_{H5,H6'}$ = 2.1 Hz, H-6′), 3.79–3.75 (1H, m, H-5), 2.12 (3H, s, OAc), 2.10 (3H, s, OAc), 2.04 (3H, s, OAc), 2.02 (3H, s, OAc), 2.15–2.10 (2H, m, H-7), 0.90 (3H, t, $J_{H8,H7}$ = 7.4 Hz, H-8) ppm. ^{13}C NMR (125 MHz, $CDCl_3$) δ: 174.1, 171.5, 170.9, 169.8, 169.5, 92.9, 73.2, 72.8, 67.9, 61.8, 53.1, 30.0, 21.1, 21.0, 20.9, 20.8, 10.1 ppm.

*1,3,4,6-Tetra-O-acetyl-2-deoxy-2-N-butyl-β-D-glucopyranose (**7c**)*—^{1}H NMR (500 MHz, $CDCl_3$) δ: 5.73 (1H, d, $J_{H1,H2}$ = 8.8 Hz, H-1), 5.58 (1H, d, $J_{NH,H2}$ = 9.5 Hz, NH), 5.21–5.14 (2H, m, H-3/H-4), 4.38 (1H, ddd, H-2), 4.31 (1H, dd, $J_{H6,H6'}$ = 12.5 Hz, H-6), 4.16 (1H, dd, $J_{H5,H6'}$ = 2.2 Hz, H-6′), 3.84 (1H, ddd, $J_{H5,H6}$ = 4.7 Hz, H-5), 2.16 (3H, s, OAc), 2.13 (3H, s, OAc), 2.18–2.10 (2H, m, H-7), 2.08 (3H, s, OAc), 2.05 (3H, s, OAc), 1.64 (2H, ddd, H-8), 0.94 (3H, t, $J_{H8,H9}$ = 7.4 Hz, H-9) ppm. ^{13}C NMR (125 MHz, $CDCl_3$) δ: 173.1, 171.4, 170.9, 169.8, 169.5, 92.9, 73.2, 72.8, 67.9, 61.9, 53.0, 38.8, 21.1, 21.0, 20.9, 20.8, 19.2, 13.7 ppm.

*1,3,4,6-Tetra-O-acetyl-2-deoxy-2-N-pentyl-β-D-glucopyranose (**7d**)*—^{1}H NMR (500 MHz, $CDCl_3$) δ: 5.68 (1H, d, $J_{H1,H2}$ = 8.8 Hz, H-1), 5.50 (1H, d, $J_{NH,H2}$ = 9.5 Hz, NH), 5.18–5.12 (2H, m, H-3/H-4), 4.36–4.30 (1H, m, H-2), 4.26 (1H, dd, $J_{H6,H6'}$ = 12.5 Hz, H-6), 4.13 (1H, dd, $J_{H5,H6'}$ = 2.2 Hz, H-6′), 3.82–3.77 (1H, m, $J_{H5,H6}$ = 4.5 Hz, H-5), 2.11 (3H, s, OAc), 2.11 (2H, m, H-7), 2.09 (3H, s, OAc), 2.04 (3H, s, OAc), 2.02 (3H, s, OAc), 1.56 (2H, dd, $J_{H7,H8}$ = 7.5 Hz, H-8), 1.52 (2H, dd, $J_{H7',H8}$ = 7.5 Hz, H-8), 1.26 (2H, ddq, $J_{H8,H9}$ = 7.5 Hz, H-9), 0.94 (3H, dd, $J_{H9,H10}$ = 7.5 Hz, H-10) ppm. ^{13}C NMR (125 MHz, $CDCl_3$) δ: 173.4, 171.4, 170.9, 169.8, 169.5, 92.9, 73.2, 72.7, 67.9, 61.9, 53.0, 36.7, 27.9, 22.4, 21.1, 21.0, 20.9, 20.8, 13.9 ppm.

*1,3,4,6-Tetra-O-acetyl-2-deoxy-2-N-hexyl-β-D-glucopyranose (**7e**)*—^{1}H NMR (500 MHz, $CDCl_3$) δ: 5.69 (1H, d, $J_{H1,H2}$ = 8.8 Hz, H-1), 5.52 (1H, d, $J_{NH,H2}$ = 9.5 Hz, NH), 5.14 (2H, m, H-3/H-4), 4.37–4.30 (1H, m, H-2), 4.26 (1H, dd, $J_{H6,H6'}$ = 12.5 Hz, H-6), 4.15–4.08 (1H, m, H-6′), 3.82–3.77 (1H, m, $J_{H5,H6}$ = 4.7 Hz, H-5), 2.11 (3H, s, OAc), 2.09 (3H, s, OAc), 2.04 (3H, s, OAc), 2.02 (3H, s, OAc), 1.58–1.52 (2H, m, H-7), 1.33–1.08 (6H, m, H-8, H-9, H-10), 0.87 (3H, t, $J_{H11,H10}$ = 7.1 Hz, H-11) ppm. ^{13}C NMR (125 MHz, $CDCl_3$) δ: 173.4, 171.4, 170.9, 169.8, 169.5, 92.9, 73.2, 72.8, 67.9, 61.9, 60.6, 53.0, 36.9, 31.4, 25.5, 22.5, 21.1, 21.0, 20.9, 20.8, 14.1 ppm.

*1,3,4,6-Tetra-O-acetyl-2-deoxy-2-N-isobutyl-β-D-glucopyranose (**7f**)*—^{1}H NMR (500 MHz, $CDCl_3$) δ: 5.70 (1H, d, $J_{H1,H2}$ = 8.8 Hz, H-1), 5.58 (1H, d, $J_{NH,H2}$ = 9.6 Hz, NH), 5.18–5.12 (2H, m, H-3/H-4), 4.36–4.30 (1H, m, H-2), 4.27 (1H, dd, $J_{H6,H6'}$ = 12.5 Hz, H-6), 4.12 (1H, dd, $J_{H5,H6'}$ = 2.2 Hz, H-6′), 3.84–3.87 (1H, m, $J_{H5,H6}$ = 4.8 Hz, H-5), 2.10 (3H, s, OAc), 2.08 (3H, s, OAc), 2.28 (1H, m, H-7), 2.04 (3H, s, OAc), 2.03 (3H, s, OAc), 1.08 (6H, t, $J_{H8,H7}$ = 2.8 Hz, H-8) ppm. ^{13}C NMR (125 MHz, $CDCl_3$) δ: 177.2, 171.5, 170.9, 169.8, 169.5, 93.0, 73.3, 72.7, 67.9, 61.9, 52.9, 36.0, 21.0, 21.0, 20.8, 20.8, 19.6 ppm.

*1,3,4,6-Tetra-O-acetyl-2-deoxy-2-N-isopentyl-β-D-glucopyranose (**7g**)*—^{1}H NMR (500 MHz, $CDCl_3$) δ: 5.67 (1H, d, $J_{H1,H2}$ = 8.8 Hz, H-1), 5.58 (1H, d, $J_{NH,H2}$ = 9.5 Hz, NH), 5.18–5.10 (2H, m, H-3/H-4), 4.38–4.32 (1H, m, H-2), 4.27 (1H, dd, $J_{H6,H6'}$ = 12.5 Hz, H-6), 4.12 (1H, dd, $J_{H5,H6'}$ = 2.2 Hz, H-6′), 3.82–3.78 (1H, m, $J_{H5,H6}$ = 4.6 Hz, H-5), 2.10 (3H, s, OAc), 2.08 (3H, s, OAc), 2.06–2.01 (2H, m, H-7), 2.04 (3H, s, OAc), 2.03 (3H, s, OAc), 1.98 (1H, ddd, H-8), 0.94 (6H, d, $J_{H8,H9}$ = 6.5 Hz, H-9) ppm. ^{13}C NMR (125 MHz, $CDCl_3$) δ: 172.6, 171.4, 170.9, 169.8, 169.5, 92.9, 73.2, 72.7, 67.9, 61.8, 52.8, 46.2, 26.3, 22.4, 22.3, 21.1, 21.0, 20.9, 20.8 ppm.

General Procedure for the Synthesis of 3,4,6-Tri-O-acetyl-1,2-dideoxy-2′-alkyl-α-D-glucopyranoso-[2,1-d]-Δ2′-thiazolines (3,4,6-Tri-O-acetyl-NAG-thiazoline Analogues)—Lawesson's Reagent (0.6 eq) was added to a solution of the appropriate 1,3,4,6-tetra-*O*-acetyl-2-*N*-acyl-2-deoxy-β-D-glucopyranose (**7a–g**) in anhydrous toluene, and the reaction mixture was refluxed for 2 h, after which time the reaction was judged to be complete by TLC analysis. The solution was cooled to room temperature, and the solvent was removed *in vacuo*. The residue was dissolved in toluene, and the desired material was isolated by flash column silica chromatography using a solvent system of hexanes and ethyl acetate in ratios ranging from 4:1 to 1:2 as appropriate. Products were isolated in yields ranging from 62 to 83%. 3,4,6-Tri-*O*-acetyl-1,2-dideoxy-2′-ethyl-α-D-glucopyranoso-[2,1-d]-Δ2′-thiazoline (**8a**) was prepared previously by using similar reaction conditions as described above (28). All spectral characterization agreed with the literature values.

*3,4,6-Tri-O-acetyl-1,2-dideoxy-2′-ethyl-α-D-glucopyranoso-[2,1-d]-Δ2′-thiazoline (**8b**)*—^{1}H NMR (500 MHz, $CDCl_3$) δ: 6.28 (1H, d, $J_{H1,H2}$ = 7.4 Hz, H-1), 5.60 (1H, dd, $J_{H3,H4}$ = 3.3 Hz, H-3), 4.97 (1H, d, $J_{H4,H5}$ = 9.3 Hz, H-4), 4.56–4.52 (1H, m, H-2), 4.18–4.10 (2H, m, H-6/H-6′), 3.58 (1H, ddd, $J_{H5,H6}$ = 3.2 Hz, H-5), 2.74–2.67 (1H, m, H-7), 2.14 (3H, s, OAc), 2.11 (3H, s, OAc), 2.09 (3H, s, OAc), 1.29 (3H, t, $J_{H8,H7}$ = 7.60 Hz, H-8) ppm.

*3,4,6-Tri-O-acetyl-1,2-dideoxy-2′-propyl-α-D-glucopyranoso-[2,1-d]-Δ2′-thiazoline (**8c**)*—^{1}H NMR (500 MHz, $CDCl_3$) δ: 6.26 (1H, d, $J_{H1,H2}$ = 7.2 Hz, H-1), 5.58 (1H, dd, $J_{H3,H4}$ = 3.3 Hz, H-3), 4.96 (1H, d, $J_{H4,H5}$ = 9.2 Hz, H-4), 4.54–4.50 (1H, m, H-2), 4.16–4.08 (2H, m, H-6/H-6′), 3.58 (1H, ddd, $J_{H5,H6}$ = 3.3 Hz, H-5), 2.70–2.58 (2H, m, H-7), 2.14 (3H, s, OAc), 2.08 (3H, s, OAc), 2.07 (3H, s, OAc), 1.76–1.69 (2H, m, H-8), 1.00 (3H, t, $J_{H9,H8}$ = 7.4 Hz, H-9) ppm.

*3,4,6-Tri-O-acetyl-1,2-dideoxy-2′-butyl-α-D-glucopyranoso-[2,1-d]-Δ2′-thiazoline (**8d**)*—^{1}H NMR (500 MHz, $CDCl_3$) δ: 6.21 (1H, d, $J_{H1,H2}$ = 7.2 Hz, H-1), 5.57 (1H, dd, $J_{H3,H4}$ = 3.3 Hz, H-3), 4.94 (1H, d, $J_{H4,H5}$ = 9.4 Hz, H-4), 4.48–4.44 (1H, m, H-2), 4.12–4.07 (2H, m, H-6/H-6′), 3.53 (1H, ddd, $J_{H5,H6}$ = 3.0 Hz, H-5), 2.60–2.57 (2H, m, H-7), 2.12 (3H, s, OAc), 2.07 (6H, s, OAc), 1.67–1.63 (2H, m, H-8), 1.40 (2H, ddd, $J_{H9,H8}$ = 7.3 Hz, H-9), 0.92 (3H, t, $J_{H10,H9}$ = 7.4 Hz, H-10) ppm.

*3,4,6-Tri-O-acetyl-1,2-dideoxy-2′-pentyl-α-D-glucopyranoso-[2,1-d]-Δ2′-thiazoline (**8e**)*—^{1}H NMR (500 MHz, $CDCl_3$) δ: 6.24 (1H, d, $J_{H1,H2}$ = 7.2 Hz, H-1), 5.60 (1H, s, H-3), 4.96 (1H, d, $J_{H4,H5}$ = 9.4 Hz, H-4), 4.52–4.49 (1H, m, H-2), 4.14–4.10 (2H, m, $J_{H6,H6'}$ = 12.2 Hz H-6/H-6′), 3.56 (1H, ddd, $J_{H5,H6}$ = 3.1 Hz, $J_{H5,H6'}$ = 5.6 Hz, H-5), 2.65–2.60 (2H, m, H-7), 2.14 (3H, s, OAc), 2.09 (3H, s, OAc), 2.08 (3H, s, OAc), 1.71–1.68 (2H, m, H-8), 1.38–1.33 (4H, m, H-9/H-10), 0.91 (3H, t, $J_{H11,H10}$ = 6.9 Hz, H-11) ppm.

*3,4,6-Tri-O-acetyl-1,2-dideoxy-2′-isopropyl-α-D-glucopyranoso-[2,1-d]-Δ2′-thiazoline (**8f**)*—^{1}H NMR (500 MHz, $CDCl_3$) δ: 6.27 (1H, d, $J_{H1,H2}$ = 7.2 Hz, H-1), 5.60 (1H, m, H-3), 4.97 (1H, d, $J_{H4,H5}$ = 9.3 Hz, H-4), 4.55–4.49 (1H, m, H-2), 4.18–4.11 (2H, m, H-6/H-6′), 3.60 (1H, ddd, $J_{H5,H6}$ = 3.1 Hz, H-5), 2.55 (2H, s, H-7), 2.15 (3H, s, OAc), 2.09 (3H, s, OAc), 2.08 (3H, s, OAc), 1.07 (6H, t, $J_{H8,H7}$ = 6.6 Hz, H-8) ppm.

*3,4,6-Tri-O-acetyl-1,2-dideoxy-2′-isobutyl-α-D-glucopyranoso-[2,1-d]-Δ2′-thiazoline (**8g**)*—^{1}H NMR (500 MHz, $CDCl_3$) δ: 6.26 (1H, d, $J_{H1,H2}$ = 7.2 Hz, H-1), 5.60 (1H, dd, $J_{H3,H4}$ = 3.3 Hz, H-3), 4.97 (1H, d, $J_{H4,H5}$ = 9.3 Hz, H-4), 4.56–4.50 (1H, m, H-2), 4.16–4.10 (2H, m, H-6/H-6′), 3.62–3.58 (1H, m, $J_{H5,H6}$ = 3.1 Hz, H-5), 2.57–2.52 (2H, m, H-7), 2.15 (3H, s, OAc), 2.09 (3H, s, OAc), 2.08 (3H, s, OAc), 2.08–2.05 (2H, m, H-8), 1.02 (6H, t, $J_{H9,H8}$ = 6.6 Hz, H-9) ppm.

General Procedure for the Synthesis of 1,2-Dideoxy-2′-alkyl-α-D-glucopyranoso-[2,1-d]-Δ2′-thiazolines (NAG-thiazoline Analogues)—A spatula tip of anhydrous sodium methoxide was added to a solution of the appropriate protected thiazoline (**8a–g**) in dry methanol. The basic solution was stirred until the reaction was judged complete by TLC analysis (typically 2 h). A solution of glacial acetic acid in methanol (1:20) was added dropwise to the reaction mixture until the pH of the solution was found to be neutral. The solvent was then removed *in vacuo*, and the desired materials (**9a–g**) were isolated by flash column silica chromatography using a solvent system of ethyl acetate and methanol in ratios ranging from 2:1 to 6:1 as appropriate. Products were isolated in yields ranging from 86 to 99%. 1,2-Dideoxy-2′-ethyl-α-D-glucopyranoso-[2,1-d]-Δ2′-thiazoline (**9a**) was prepared previously using similar reaction conditions as described above (30). All spectral characterization agreed with the literature values as did the elemental analysis of the sample used in these assays.

$C_8\ H_{13}\ O_4\ NS$

Calculated:	C 43.82	H 5.98	N 6.39
Found:	C 43.45	H 6.23	N 6.18

*1,2-Dideoxy-2′-ethyl-α-D-glucopyranoso-[2,1-d]-Δ2′-thiazoline (**9b**)*—^{1}H NMR (500 MHz, CD_3OD) δ: 6.31 (1H, d, $J_{H1,H2}$ = 7.0 Hz, H-1), 4.29–4.26 (1H, m, $J_{H2,H3}$ = 4.32 Hz, H-2), 4.09 (1H, dd, $J_{H3,H4}$ = 4.32 Hz, H-3), 3.70 (1H, dd, $J_{H6,H6'}$ = 12.07 Hz, H-6), 3.57 (1H, dd, H-6′) 3.52 (1H, dd, $J_{H4,H5}$ = 9.10 Hz, H-4), 3.32–3.29 (1H, m, $J_{H5,H6}$ = 6.29 Hz, $J_{H5,H6'}$ = 2.21 Hz, H-5), 2.52 (2H, dd, $J_{H7,H8}$ = 7.59 Hz, H-7), 1.18 (3H, t, H-8) ppm. ^{13}C NMR (125 MHz, CD_3OD) δ: 175.1, 89.4, 80.2, 75.7, 74.5, 71.4, 62.5, 28.9, 11.1 ppm;

$C_9\ H_{15}\ O_4\ NS$

Calculated:	C 46.34	H 6.48	N 6.00
Found:	C 45.95	H 6.33	N 5.93

*1,2-Dideoxy-2′-propyl-α-D-glucopyranoso-[2,1-d]-Δ2′-thiazoline (**9c**)*—^{1}H NMR (500 MHz, CD_3OD) δ: 6.32 (1H, d, $J_{H1,H2}$ = 7.0 Hz, H-1), 4.28 (1H, m, $J_{H2,H3}$ = 4.4 Hz, H-2), 4.09 (1H, dd, $J_{H3,H4}$ = 4.4 Hz, H-3), 3.72 (1H, dd, $J_{H6,H6'}$ = 12.0 Hz, H-6), 3.59 (1H, dd, H-6′), 3.53 (1H, dd, $J_{H4,H5}$ = 9.1 Hz, H-4), 3.33 (1H, m, $J_{H5,H6}$ = 6.3 Hz, $J_{H5,H6'}$ = 2.5 Hz, H-5), 2.51–2.48 (1H, m, $J_{H7,H8}$ = 7.3 Hz, $J_{H7,H7'}$ = 14.9 Hz, H-7), 2.49–2.47 (1H, m, H-7′), 1.68–1.65 (2H, m, $J_{H8,H9}$ = 7.4 Hz, H-8) 0.98 (3H, dd, H-9);

$C_{10}\ H_{17}\ O_4\ NS$

Calculated:	C 48.57	H 6.93	N 5.66
Found:	C 48.32	H 6.77	N 5.45

*1,2-Dideoxy-2′-butyl-α-D-glucopyranoso-[2,1-d]-Δ2′-thiazoline (**9d**)*—^{1}H NMR (500 MHz, CD_3OD) δ: 6.31 (1H, d, $J_{H1,H2}$ = 7.0 Hz, H-1), 4.30–4.28 (1H, m, $J_{H2,H3}$ = 4.4 Hz, H-2), 4.09 (1H, dd, $J_{H3,H4}$ = 4.4 Hz, H-3), 3.71 (1H, dd, $J_{H6,H6'}$ = 12.0 Hz, H-6), 3.59 (1H, dd, H-6′), 3.53 (1H,

dd, $J_{H4,H5}$ = 9.1 Hz, H-4), 3.35–3.30 (1H, m, $J_{H5,H6}$ = 6.3 Hz, $J_{H5,H6'}$ = 2.5 Hz, H-5), 2.58–2.53 (1H, m, $J_{H7,\ H8}$ = 7.8 Hz, $J_{H7,H7'}$ = 14.8 Hz, H-7) 2.53–2.50 (1H, m, $J_{H7',H8}$ = 7.6 Hz, H-7′) 1.60 (2H, ddd, $J_{H8,H9}$ = 14.9 Hz, H-8) 1.37 (2H, ddd, $J_{H9,H10}$ = 7.4, H-9) 0.92 (3H, t, H-10) ppm. ^{13}C NMR (125 MHz, CD_3OD) δ: 175.5, 89.4, 79.1, 75.2, 74.2, 71.5, 62.7, 36.9, 20.4, 15.2 ppm;

$C_{11}\ H_{19}\ O_4\ NS$

Calculated:	C 50.55	H 7.33	N 5.36
Found:	C 50.68	H 7.12	N 5.13

1,2-Dideoxy-2′-pentyl-α-D-glucopyranoso-[2,1-d]-Δ2′-thiazoline (***9e***)—^{1}H NMR (500 MHz, CD_3OD) δ: 6.20 (1H, d, $J_{H1,H2}$ = 6.9 Hz, H-1), 4.29–4.27 (1H, m, $J_{H2,H3}$ = 6.0 Hz, H-2), 4.09 (1H, dd, $J_{H3,H4}$ = 4.4 Hz, H-3), 3.72 (1H, dd, $J_{H6,H6'}$ = 12.0 Hz, H-6), 3.59 (1H, dd, H-6′), 3.53 (1H, dd, $J_{H4,H5}$ = 9.1 Hz, H-4), 3.35–3.31 (1H, m, $J_{H5,H6}$ = 6.3, $J_{H5,H6'}$ = 2.4 Hz, H-5), 2.52 (2H, ddd, $J_{H7,H8}$ = 6.2 Hz, H-7), 1.37–1.32 (2H, m, H-8), 1.35–1.30 (2H, m, H-9), 1.66–1.63 (2H, m, $J_{H10,H11}$ = 7.1 Hz, H-10), 0.90 (3H, t, H-11) ppm. ^{13}C NMR (125 MHz, CD_3OD) δ: 174.8, 89.3, 79.2, 75.5, 73.4, 71.5, 62.2, 35.4, 30.3, 28.8, 22.1, 13.1 ppm;

$C_{12}\ H_{21}\ O_4\ NS$

Calculated:	C 52.34	H 7.69	N 5.09
Found:	C 52.48	H 7.67	N 4.40

1,2-Dideoxy-2′-isopropyl-α-D-glucopyranoso-[2,1-d]-Δ2′-thiazoline (***9f***)—^{1}H NMR (500 MHz, CD_3OD) δ: 6.31 (1H, d, $J_{H1,H2}$ = 7.0 Hz, H-1), 4.29 (1H, m, $J_{H2,H3}$ = 4.4 Hz, H-2), 4.11 (1H, dd, $J_{H3,H4}$ = 4.4 Hz, H-3), 3.60 (1H, dd, $J_{H6,H6'}$ = 12.0 Hz, H-6), 3.72 (1H, dd, H-6′), 3.55 (1H, dd, $J_{H4,H5}$ = 9.1 Hz, H-4), 3.35–3.32 (1H, m, $J_{H5,H6}$ = 6.4 Hz, $J_{H5,H6'}$ = 2.4 Hz, H-5), 2.87–2.83 (2H, m, $J_{H7,H8}$ = 6.9 Hz, H-7), 1.24 (3H, d, H-8), 1.21 (3H, d, H-8′) ppm. ^{13}C NMR (125 MHz, CD_3OD) δ: 175.2, 89.5, 79.7, 75.6, 72.3, 70.8, 62.3, 35.1, 30.3, 22.5, 13.8 ppm;

$C_{10}\ H_{17}\ O_4\ NS$

Calculated:	C 48.57	H 6.93	N 5.66
Found:	C 48.40	H 6.70	N 5.33

1,2-Dideoxy-2′-isobutyl-α-D-glucopyranoso-[2,1-d]-Δ2′-thiazoline (***9g***)—^{1}H NMR (500 MHz, CD_3OD) δ: 6.38 (1H, d, $J_{H1,H2}$ = 7.1 Hz, H-1), 4.28–4.24 (1H, m, $J_{H2,H3}$ = 6.0 Hz, H-2), 4.06 (1H, dd, $J_{H3,H4}$ = 6.0 Hz, H-3), 3.71 (1H, dd, $J_{H6,H6'}$ = 12.0 Hz, H-6), 3.58 (1H, dd, H-6′), 3.58 (1H, dd, $J_{H4,H5}$ = 9.2 Hz, H-4), 3.35–3.30 (1H, m, $J_{H5,H6}$ = 6.3 Hz, $J_{H5,H6'}$ = 2.4 Hz, H-5), 2.46–2.40 (1H, m, $J_{H7,H8}$ = 7.3 Hz, $J_{H7,H7'}$ = 14.1 Hz, H-7) 2.37–2.33 (1H, m, $J_{H7',H8}$ = 7.3 Hz, H-7′) 2.00 (2H, ddd, $J_{H8,H9}$ = 6.7 Hz, H-8) 0.97 (3H, d, H-9) 0.96 (3H, d, H-9′) ppm;

$C_{11}\ H_{19}\ O_4\ NS$

Calculated:	C 50.55	H 7.33	N 5.36
Found:	C 50.68	H 7.12	N 5.13

Cell Culture and Inhibition—COS-7 cells were cultured in Dulbecco's modified Eagle's medium (Invitrogen) supplemented with 5–10% fetal bovine serum (Invitrogen). Aliquots of inhibitors (50 μl of a stock in 95% ethanol) were delivered onto tissue culture plates, and the ethanol was evaporated. The cells were incubated at 37 °C for 40 h at which time they reached ~80% confluence. The time-dependent accumulation of *O*-GlcNAc-modified proteins in response to treatment with 50 μM of compound **9c** cells was studied as follows. COS-7 cells were cultured to 25% confluence in 5% fetal bovine serum, and an aliquot (100 μl) of inhibitor dissolved in media and filter-sterilized was added to each plate to yield a final concentration of 50 μM of inhibitor. COS-7 cells (2 × 10-cm plates) were harvested at the appropriate times by scraping and were pooled by centrifugation (200 × *g*, 10 min). Cells were washed once with PBS, pH 7.0 (10 ml), and pelleted (200 × *g*, 10 min). The cells could be frozen at −80 °C at this point. Control cultures without inhibitor were treated in the same manner.

Western Blot Analyses—COS-7 cells were cultured in the presence of inhibitors **9a**, **9c**, or **9g** as described above to ~90% of confluence. A culture of control cells was treated in the same manner as follows, but the cultures contained no inhibitor. Cells were harvested as described above. Frozen cells were thawed at 4 °C, and cold lysis buffer (1 ml of 50 mM Tris, pH 8.0, containing 150 mM NaCl, 1 mM EDTA, 1 mM phenylmethylsulfonyl fluoride, 1% Nonidet P-40, 0.5% sodium deoxycholate, and 1 mM of inhibitor **9f**) was added. After 10 min at 4 °C, the solution was centrifuged at 14,000 rpm in an Eppendorf 5415C microcentrifuge, and the supernatant was collected. SDS-PAGE loading buffer was added to an aliquot (15 μl) of each sample, and after heating at 96 °C aliquots were loaded onto 10 or 12% Tris·HCl polyacrylamide gels. After electrophoresis, the samples were electroblotted to nitrocellulose membrane (0.45 μm, Bio-Rad). Transfer was verified by visual inspection of the transfer of prestained markers (Dual Color Precision Plus Protein Standard, Bio-Rad). The membrane was blocked by using 5% BSA (fraction V, Sigma) in PBS (blocking buffer A for samples probed with mouse anti-*O*-GlcNAc monoclonal IgM antibody (mAb CTD 110.6, Covance)) or 5% low-fat dry powdered milk (blocking buffer B for samples probed with anti-β-actin), pH 7.4, containing 0.1% Tween 20 for 1 h at room temperature or overnight at 4 °C. The blocking solution was decanted, and a solution of blocking buffer A containing mAb CTD 110.6 (1:2500 of the stock) or blocking buffer B containing mouse monoclonal anti-β-actin IgG (clone AC-40, Sigma) was added (1:1000 dilution) as appropriate. The membrane was incubated at room temperature for 1 h or overnight at 4 °C after which the blocking buffer was decanted, and the membrane was rinsed with PBS, pH 7.4, containing 0.1% Tween 20 (wash buffer). Membranes were then rinsed two times for 5 min and three times for 15 min with wash buffer. For immunological detection of *O*-GlcNAc, the membrane was incubated in blocking buffer A for 1 h at room temperature, and after washing, the membrane was incubated with a secondary goat anti-mouse-IgM-HRP conjugate (1:2500, Santa Cruz Biotechnology) for 1 h at room temperature or 4 °C overnight in blocking solution. For detection of β-actin levels, the membrane was incubated with a secondary goat anti-mouse IgG-HRP conjugate (1:100,000, Sigma) for 1 h at room temperature or 4 °C overnight in blocking solution B. Membranes were washed, and detection of membrane-bound goat anti-mouse IgG-HRP conjugate was accomplished by chemiluminescent detection using the SuperSignal West Pico chemiluminescent detection kit (Pierce) and film (Kodak Biomax MR).

RESULTS AND DISCUSSION

Comparative Analysis of the Catalytic Mechanisms of O-GlcNAcase and β-Hexosaminidase—Three realistic mechanistic alternatives exist for *O*-GlcNAcase and family 84 glycoside hydrolases. The first alternative is an inverting mechanism (Fig. 1*A*) such as that found for goose lysozyme (53) from family 23 of glycoside hydrolases. This catalytic mechanism generally involves the nucleophilic attack of water at the anomeric center concomitant with the acid-catalyzed departure of the leaving group. The second mechanistic possibility is the canonical two-step double displacement mechanism that results in retention of configuration at the anomeric center (Fig. 1*B*). This mechanism is used by most retaining β-glycosidases and involves, in the first step, attack of an enzymatic nucleophile at the anomeric center with the resulting formation of a transient covalent glycosyl enzyme intermediate (54). Departure of the aglycon leaving group is facilitated by an enzymatic residue acting as a catalytic general acid. In the second step this same residue acts as a catalytic general base to facilitate the attack of a water molecule at the anomeric center, cleaving the intermediate to liberate the hemiacetal product with retained stereochemistry. β-*N*-Acetylglucosaminidases from family 3 of glycoside hydrolases have been shown to use this mechanism (55) as have the C-type lysozymes from family 22 (56). The third mechanistic alternative involves the nucleophilic participation of the 2-acetamido group of the substrate in place of an enzymatic catalytic nucleophile (Fig. 1*C*). This last mechanistic option is exploited by β-hexosaminidases from family 20 of glycoside hydrolases (30, 57, 58). These three mechanisms differ in several aspects. The inverting mechanism is a one-step reaction that results in the formation of a product with inverted stereochemistry at the anomeric center. The other two alternatives are retaining in stereochemistry at the anomeric center and differ from each other primarily in the nature of the intermediate; in the second mechanism this species is a covalent enzyme adduct, whereas in the third case it is believed to be a bicyclic oxazoline or oxazolinium ion.

A key difference between these mechanistic alternatives is

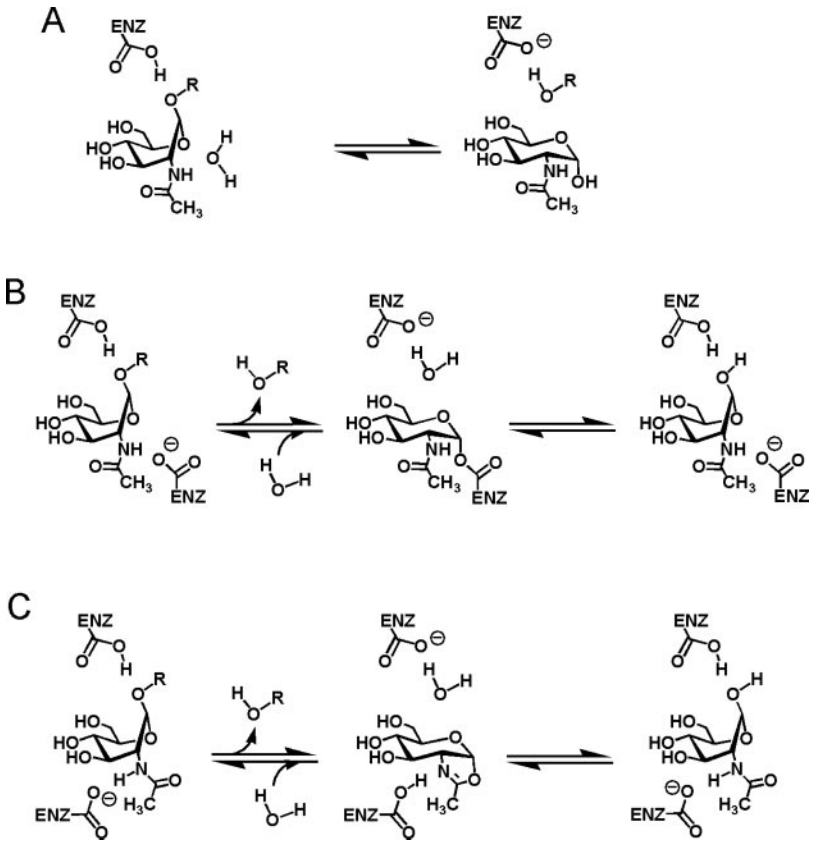

FIG. 1. **Three possible catalytic mechanisms for *O*-GlcNAcase.** *A*, the single step inverting mechanism; *B*, the double displacement retaining mechanism involving formation and breakdown of a covalent glycosyl enzyme intermediate; *C*, the double displacement retaining mechanism involving formation and breakdown of a bicyclic oxazoline intermediate. *ENZ*, enzyme.

the involvement of the 2-acetamido group of the substrate. This moiety may actively participate in catalysis as a nucleophile, as for the lysosomal β-hexosaminidases, or it may act as a bystander. To address the role of the 2-acetamido group of the substrate, we synthesized several substrate analogues bearing differing levels of fluorine substitution on the *N*-acetyl group (Scheme 1). The highly electronegative fluorine substituents decrease the basicity of the carbonyl group, and the expected effect of such substitutions on an enzymatic reaction using anchimeric assistance would be to decrease its rate. These compounds were first tested with the lysosomal human β-hexosaminidase because this enzyme is known to proceed via a mechanism involving anchimeric assistance (Fig. 1*C*). Although Michaelian saturation kinetics were not observed for all substrates (Table I), $V_{max}/[E]_0K_M$, which is proportional to the second order rate constant governing the enzyme-catalyzed reaction, could be determined from the initial slope of the Michaelis-Menten plot (Fig. 2*A*, *inset*). A plot of log $V_{max}/[E]_0K_M$ against the Taft electronic parameter (σ^*) of the *N*-acyl substituent shows a negative linear correlation on increasing fluorine substitution (Fig. 2*C*). As expected, decreasing the basicity of the carbonyl oxygen has a deleterious effect on catalysis. The steep negative slope of the Taft-like linear free energy analysis (given by the reaction constant, $\rho = -1.0 \pm 0.1$) suggests that the carbonyl oxygen acts as a nucleophile, attacking the anomeric center. The data are consistent with a mechanism involving electrophilic migration of the anomeric center and consequent oxocarbenium-ion like transition states that have been generally proposed for enzyme-catalyzed glycoside hydrolysis (54, 56). For *O*-GlcNAcase, Michaelian saturation kinetics were observed for all four substrates; therefore, both kinetic parameters were determined (Table I and Fig. 2*B*). For *O*-GlcNAcase, the value of $V_{max}/[E]_0K_M$ is also dependent on the extent of fluorine substitution, but the slope is more shallow ($\rho = -0.42 \pm 0.08$, Fig. 2*C*). On the basis of these results,

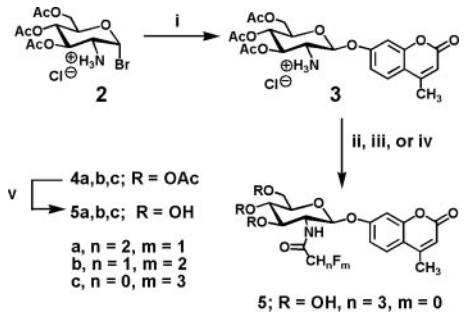

SCHEME 1. **(*i*) *a*, acetone, 4-MU, Na4-MU; *b*, K_2CO_3, Et_2O; *c*, HCl; (*ii*) *a*, Dowex 50-H^+, $NaOOCCH_2F$; *b*, DMF, Et_3N, Py, DCC, 4 °C; (*iii*) DMF, Et_3N, Py, DCC, $F_2HCCOOH$, 4 °C; (*iv*) DMF, Et_3N, Py, DCC, $(F_3CCO)_2O$, 4 °C; (*v*) *a*, NaOMe, MeOH; *b*, Dowex 50-H^+.**

it appears that *O*-GlcNAcase, in common with lysosomal β-hexosaminidase, uses a catalytic mechanism involving anchimeric assistance.

The reaction constant (ρ), which is the slope of the correlations in the Taft-like analyses, is an indication of the sensitivity of the reaction to different substituents. This constant can be considered a function of both an electronic component (ρ^*, which is governed by sensitivity of the reaction to the electronic parameter of the substituents, σ^*) and a steric component (δ, which is governed by sensitivity of the reaction to the steric Taft parameters of the substituent, E_s) according to Equation 1,

$$\rho = \rho^* + \delta \qquad \text{(Eq. 1)}$$

The difference between the slopes measured for lysosomal β-hexosaminidase and *O*-GlcNAcase may thus reflect the position of the transition state along the reaction coordinate or may indicate that the lysosomal β-hexosaminidase has a more sterically constrained active site architecture than does *O*-GlcNAcase. Indeed, a common misconception is that fluorine

TABLE I
Michaelis-Menten parameters for the β-hexosaminidase and O-GlcNAcase-catalyzed hydrolysis of a series of 4-methylumbelliferone 2-N-acetyl-2-deoxy-β-D-glucopyranosides

Substrate	σ^{*a}	Enzyme	K_M	$V_{max}/[E]_0$	$V_{max}/[E]_0K_M$
			mM	*μmol min^{-1} mg^{-1}*	*μmol mM^{-1} min^{-1} mg^{-1}*
MuGlcNAc (**5**)	0.0	Hexosaminidase	0.88 ± 0.05	8.3 ± 0.2	9.5 ± 0.8
		O-GlcNAcase	0.43 ± 0.04	0.74 ± 0.02	1.7 ± 0.2
MuGlcNAc-F_1 (**5a**)	0.8	Hexosaminidase	3.8 ± 0.4[b]	3.3 ± 0.2[b]	0.40 ± 0.07[c]
		O-GlcNAcase	0.49 ± 0.06	0.60 ± 0.03	1.2 ± 0.2
MuGlcNAc-F_2 (**5b**)	2.0	Hexosaminidase	ND[d]	ND[d]	0.069 ± 0.001[c]
		O-GlcNAcase	0.45 ± 0.05	0.16 ± 0.01	0.36 ± 0.06
MuGlcNAc-F_3 (**5c**)	2.8	Hexosaminidase	ND[d]	ND[d]	0.0077 ± 0.0010[c]
		O-GlcNAcase	0.38 ± 0.03	0.033 ± 0.001	0.0077 ± 0.0008

[a] The Taft electronic parameters (σ^*) used for each *N*-acyl substituent were obtained from Hansch and Leo (66).
[b] Values were estimated by nonlinear regression of the Michaelis-Menten data. Note that substrate concentrations assayed matched but did not exceed K_M due to limited substrate solubility.
[c] Values were determined by linear regression of the second order region of the Michaelis-Menten plot.
[d] These values could not be determined as saturation kinetics were not observed because of limitations in substrate solubility.

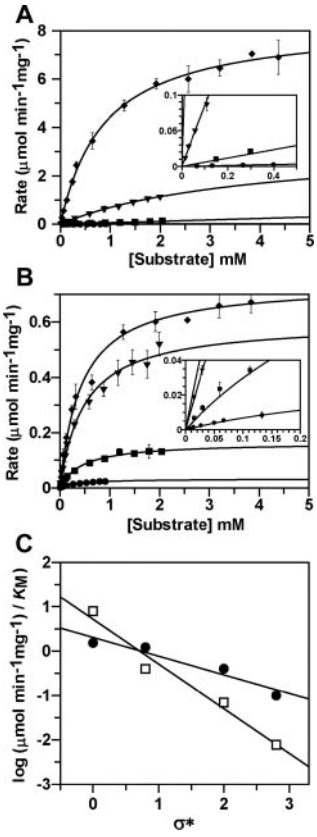

FIG. 2. **Activity of *O*-GlcNAcase and β-hexosaminidase with *N*-fluoroacetyl derivatives of MU-GlcNAc.** *A*, initial velocities of the human β-hexosaminidase-catalyzed hydrolysis of *N*-fluoroacetyl derivatives of MU-GlcNAc; ♦, MU-GlcNAc (**5**); ▼, MU-GlcNAc-F (**5a**); ■, MU-GlcNAc-F_2 (**5b**); ●, MU-GlcNAcF$_3$ (**5c**). *Inset*, detail of the region of the plot at the intersection of the axes. *B*, initial velocities of the human *O*-GlcNAcase-catalyzed hydrolysis of *N*-fluoroacetyl derivatives of MU-GlcNAc; ♦, MU-GlcNAc (**5**); ▼, MU-GlcNAc-F (**5a**); ■, MU-GlcNAc-F_2 (**5b**); ●, MU-GlcNAcF$_3$ (**5c**). *Inset*, detail of the region of the plot at the intersection of the axes. *C*, linear free energy analysis plotting the Taft parameter (σ^*) of the *N*-fluoroacetyl substituent of MU-GlcNAc substrate analogues against the log $V_{max}/[E]_0K_M$ values measured for each substrate as shown in *A* and *B* with *O*-GlcNAcase (●) and β-hexosaminidase (□).

(147 pm van der Waals radius and 138 pm C–F bond length) is often considered to have a negligible difference in size as compared with hydrogen (120 pm van der Waals radius and 109 pm C–H bond length). Therefore, it is possible that unfavorable steric interactions between the substrate and the active site of human β-hexosaminidase may play an additional role, beyond electronics, in discriminating between the varying levels of fluorine substitution. Indeed, the recent crystal structures of human hexosaminidase B revealed a carefully structured pocket that tightly nestles the acetamido group between three tryptophan residues (50, 59). For *O*-GlcNAcase, no three-dimensional structure is available. The relatively constant K_M values measured for all of the substrate analogues (Table I) suggest, however, that steric effects are not a major contributor and that the electronic effect of the *N*-acyl-fluorine substituents predominate. An earlier study of an isolated enzyme of unknown family using two *para*-nitrophenyl 2-acetamido-2-deoxy-β-D-glucopyranoside (*p*NP-GlcNAc) analogues, with either two or three fluorine substituents in the acetamido group, yielded a ρ of -1.41 ± 0.1 when log V_{max}/K_M was plotted against σ^* (60). This value is even greater than that found for the lysosomal β-hexosaminidase in this study ($\rho = -1.0 \pm 0.1$), suggesting that the enzyme Jones and Kosman (60) studied from *Aspergillus niger* is more likely a member of family 20 of glycoside hydrolases than of family 84.

Inhibition of O-GlcNAcase and β-Hexosaminidase with NAG-thiazoline—As a further test of whether *O*-GlcNAcase uses a catalytic mechanism involving anchimeric assistance, we tested the inhibitor NAG-thiazoline (**9a**) with this enzyme. NAG-thiazoline, designed as a mimic of the bicyclic oxazoline intermediate, has been demonstrated previously to function as an inhibitor of family 20 hexosaminidases (30, 57). Using *p*NP-GlcNAc (**5**) as a substrate, we found NAG-thiazoline to be a potent inhibitor of family 84 human *O*-GlcNAcase, and a clear pattern of competitive inhibition was observed (Fig. 3). Nonlinear regression revealed a K_I value of 180 nM at pH 7.4, and analysis using 4-methylumbelliferyl 2-acetamido-2-deoxy-β-D-glucopyranoside (MU-GlcNAc) revealed a K_I value of 70 nM at pH 6.5 (Table II). NAG-thiazoline is therefore a potent inhibitor of *O*-GlcNAcase, binding ~21,000-fold more tightly than the parent saccharide, GlcNAc (K_I = 1.5 mM), at pH 6.5. This potent inhibition may be attributed to the resemblance of NAG-thiazoline to a putative oxazoline intermediate or a structurally related transition state. Indeed, the observed inhibition data are similar to those measured by us for the family 20 human lysosomal β-hexosaminidase (K_I = 70 nM, 17,000-fold more tightly than GlcNAc for which the K_I value is 1.2 mM) and strongly support the Taft-like analysis indicating that *O*-GlcNAcase, in common with the family 20 β-hexosaminidases, uses a catalytic mechanism involving anchimeric assistance. Glycoside hydrolases from families 18 (61) and 56 (62), which are endoglycosidases acting to cleave oligosaccharide chains, have also been shown to use a mechanism involving anchimeric assistance (63). Thus families 18, 20, 56 and 84 are all comprised of retaining glycosidases that use a catalytic mechanism

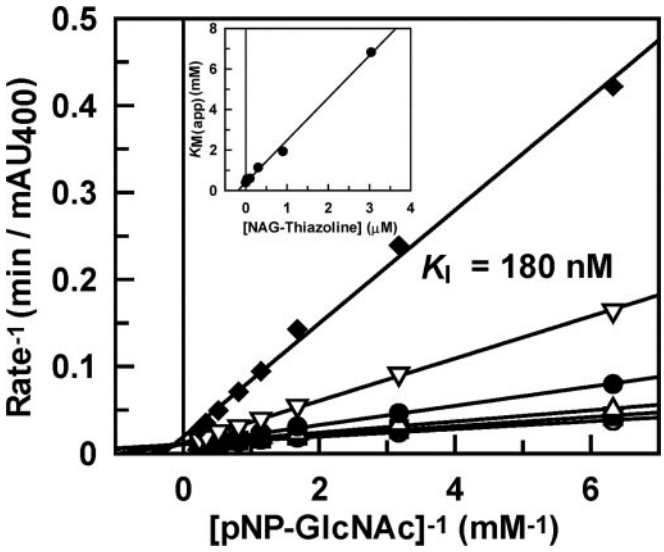

FIG. 3. **Inhibition of human *O*-GlcNAcase-catalyzed hydrolysis of *p*NP-GlcNAc (5) by NAG-thiazoline (9a) shows a pattern of competitive inhibition.** The concentrations of **9a** (μM) used were 3.04 (♦), 0.900 (▽), 0.300 (●), 0.100 (△), 0.033 (■), and 0.00 (○). *Inset*, graphical analysis of K_I from plotting K_M apparent against NAG-thiazoline (**9a**) concentration.

involving anchimeric assistance from the acetamido group of the substrate. This is in marked contrast to retaining β-glycosidases from families 3 and 22 that also act on substrates bearing an acetamido group at the 2-position of their respective substrates (55, 56) as well as the family 23 inverting endoglycosidases (53).

Design, Synthesis, and Testing of Selective O-GlcNAcase Inhibitors—With the mechanism of human *O*-GlcNAcase, and by extension other members of family 84 of glycoside hydrolases, established, we turned our attention to using this information in the design of inhibitors that would be selective for this enzyme over the human lysosomal hexosaminidases. Because both β-hexosaminidase and *O*-GlcNAcase use a mechanism involving anchimeric assistance, we chose NAG-thiazoline as a scaffold that could be elaborated to generate the required selectivity. Three observations provided a starting point in the design of the inhibitor. The first is that the slope of the Taft-like analysis for the lysosomal enzyme is much steeper than that measured for *O*-GlcNAcase, thereby suggesting that the bulk of the *N*-acyl group may be a determinant in substrate recognition (see above). The second, and related, consideration is that the structure of the human lysosomal β-hexosaminidase B reveals a snug pocket into which the methyl group of the acetamido substituent is poised (50). The third is that STZ, which bears a bulky *N*-acyl substituent, shows some selectivity for *O*-GlcNAcase over β-hexosaminidase (46).

We therefore prepared a series of seven inhibitors in which the thiazoline ring was elaborated with aliphatic chains of increasing length in the expectation that these compounds would allow the discriminative inhibition of *O*-GlcNAcase over lysosomal hexosaminidase. The synthesis of this panel of inhibitors is outlined in Scheme 2. This facile synthetic route enables the production of quantities of inhibitor from commercially available starting materials in three steps or from the inexpensive starting material 2-amino-2-deoxyglucopyranose in six steps. Analysis of the inhibition of human β-hexosaminidase reveals that increasing the chain length resulted in a marked decrease in the potency of these inhibitors (Fig. 4 and Table II). The inclusion of even one methylene unit (compound **9b**) resulted in a 460-fold increase in the value of K_I for β-hexosaminidase as compared with the parent compound NAG-thiazoline (**9a**). Further increases in the chain length lead to still greater increases in K_I values. For *O*-GlcNAcase, however, the situation is markedly different (Fig. 4 and Table II). Increases in chain length are much better tolerated, and the inclusion of two methylene units yields a compound (**9c**) for which the K_I value (K_I = 230 nM) is only 3-fold greater than that measured for the parent compound (**9a**) NAG-thiazoline (K_I = 70 nM). Branching of the aliphatic chain also does not abrogate binding because both compounds **9f** and **9g** are good inhibitors of *O*-GlcNAcase. From analysis of the data, it can be seen that compounds **9b, 9c,** and **9f** are potent inhibitors of *O*-GlcNAcase and show a remarkable selectivity for *O*-GlcNAcase over lysosomal hexosaminidase. Indeed, the selectivity ratio for *O*-GlcNAcase over β-hexosaminidase is 3100-fold for compound **9d**, 1500-fold for compound **9c**, and 700-fold for compound **9f** (Fig. 4 and Table II).

We also tested existing inhibitors of *O*-GlcNAcase for their inhibitory properties and selectivities. We determined the K_I values for STZ (Table II) with both *O*-GlcNAcase (K_I = 1.5 mM) and β-hexosaminidase (K_I = 47 mM), and we found the value measured for *O*-GlcNAcase to be consistent with previous determinations of the IC_{50} values that were in the range of 1 to 2.5 mM (42, 46). The selectivity of STZ for *O*-GlcNAcase over β-hexosaminidase is surprisingly modest (31-fold) given the bulk of the *N*-acyl group of this compound. Perhaps the thiazoline compounds demonstrate greater selectivity than STZ by virtue of the fact that they may emulate a transition state or tightly bound intermediate. We also investigated the possible STZ-induced irreversible inactivation of *O*-GlcNAcase and β-hexosaminidase. Irreversible inhibitors result in the time-dependent loss of enzyme activity as the inactivator modifies the protein. To first check the stability of STZ in aqueous solution and the purity of the commercially available material, we monitored, by NMR, the time-dependent decomposition of STZ freshly dissolved in deuterated water. STZ decomposed over time with a half-life clearly greater than 6 h. In our hands, freshly dissolved STZ did not act as a time-dependent inactivator of *O*-GlcNAcase nor of β-hexosaminidase over a period of 6 h (see the Supplemental Material).[3] The selectivity of PUGNAc was also investigated. We measured the K_I value for PUGNAc (K_I = 46 nM) with *O*-GlcNAcase, and we found it in close agreement with the value determined previously (K_I = 52 nM) (21). This compound, however, shows no selectivity for *O*-GlcNAcase as compared with β-hexosaminidase (K_I = 36 nM). It is interesting to speculate that an *N*-acyl group bulkier than an acetyl group would yield selective PUGNAc-based inhibitors. Regardless, the remarkably high selectivities of the thiazoline-containing compounds described herein should greatly facilitate finding the appropriate dose to obtain entirely selective inhibition of *O*-GlcNAcase at the organismal level.

These data also support the view, see above, that the steric bulk of the *N*-acyl group of the fluorine-substituted substrates does not contribute greatly to the slope of the Taft-like analysis (ρ = −0.42) measured with *O*-GlcNAcase. The slope (ρ = −1.0) measured with lysosomal β-hexosaminidase, however, appears likely to be a composite of both electronic and steric effects according to Equation 1. The sensitivity of the reaction to the electronic effect of the fluorine substituents (ρ^*) may therefore be the same for both enzymes, but the significant sensitivity of the lysosomal β-hexosaminidase catalyzed reaction to the steric effect of the substrates (δ) results in an apparently

[3] In our work, both *O*-GlcNAcase and β-hexosaminidase incubated with STZ showed no significant time-dependent loss of enzymatic activity when compared with a control containing no STZ (see Supplemental Material). Thus STZ does not appear to act as an irreversible inhibitor of *O*-GlcNAcase nor β-hexosaminidase.

TABLE II
Inhibition constants and selectivity of inhibitors for both O-GlcNAcase and β-hexosaminidase

Compound	*O*-GlcNAcase K_I	β-Hexosaminidase K_I	Selectivity ratio (β-Hexosaminidase K_I/*O*-GlcNAcase K_I)
	μM	μM	
GlcNAc	1500	1200	0.8
STZ	1500[a]	47,000[a]	31
PUGNAc	0.046	0.036	0.8
9a	0.070	0.070	1
9b	0.12	32	270
9c	0.23	340	1500
9d	1.5	4600	3100
9e	57	11,000	100
9f	1.6	720	700
9g	5.7	4000	190

[a] In our work, both *O*-GlcNAcase and β-hexosaminidase incubated with STZ showed no significant time-dependent loss of enzymatic activity when compared with a control containing no STZ (see Supplemental Material). Thus STZ does not appear to act as an irreversible inhibitor of *O*-GlcNAcase nor of β-hexosaminidase.

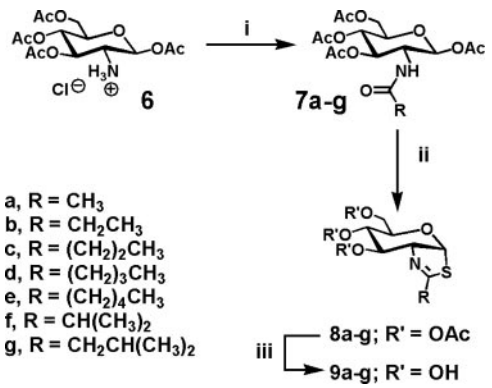

SCHEME 2. **(*i*) RCOCl, Et_3N, CH_2Cl_2, 0 °C; (*ii*) Lawesson's reagent, *Tol* (toluene), Δ; (*iii*) *a*, NaOMe, MeOH; *b*, AcOH, MeOH.**

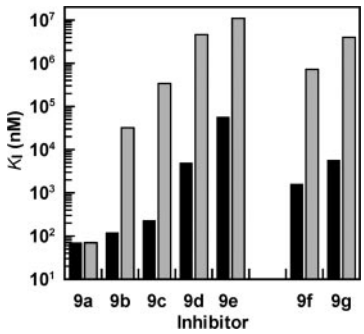

FIG. 4. **Selectivity of inhibition of *O*-GlcNAcase over β-hexosaminidase by a panel of thiazoline inhibitors.** *Bar graph* of the K_I values of the panel of thiazoline inhibitors (***9a–f***) measured for the inhibition of the *O*-GlcNAcase- (■) and β-hexosaminidase (▨)-catalyzed hydrolysis of MU-GlcNAc.

steeper slope for β-hexosaminidase than that measured for *O*-GlcNAcase. Together, the Taft-like linear free energy analyses and the selective inhibition data suggest that the active site of *O*-GlcNAcase has considerably more space in the region surrounding the 2-acetamido group of the substrate than does lysosomal β-hexosaminidase. Clarification of the precise molecular differences in the active site architectures of these two enzymes awaits structural elucidation of *O*-GlcNAcase.

Evaluation of Selective Inhibitors in Cell Culture—Having demonstrated the selectivity of these compounds *in vitro*, we now turned to evaluating their use in living cells. COS-7 cells incubated in plates with 50 μM of inhibitor **9a**, **9c**, or **9g** revealed no abnormalities in proliferation rate or morphology as compared with control cells (data not shown). Cellular *O*-GlcNAc levels within cells cultured for 40 h in the presence of inhibitors **9a**, **9c**, or **9g**, or in their absence were carried out using the *O*-GlcNAc directed monoclonal antibody (64) mAb CTD

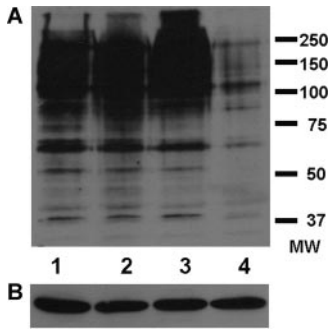

FIG. 5. **Incubation of COS-7 cells with thiazoline inhibitors causes an increase in cellular levels of *O*-GlcNAc-modified proteins.** Western blot analysis of proteins from COS-7 cells cultured for 40 h in the presence or absence of 50 μM of different thiazoline inhibitors. *Lane 1,* thiazoline **9a**; *lane 2*, thiazoline **9c**; *lane 3*, thiazoline **9g**; *lane 4*, no inhibitor. *A*, Western blot analysis of cellular *O*-GlcNAc levels using anti-*O*-GlcNAc mAb CTD 110.6 followed by an anti-mouse IgG-HRP conjugate. *B*, Western blot of samples loaded in *A* treated with anti-β-actin mAb clone AC-40 followed by an anti-mouse IgG-HRP conjugate reveals equivalent β-actin levels in each sample.

110.6. Marked increases in cellular *O*-GlcNAc levels within the cells were observed as compared with the control (Fig. 5*A*), indicating that these compounds readily gain access to the interior of the cell where they act to block *O*-GlcNAcase function. We also probed the speed with which the thiazoline inhibitor (**9c**) acts to block *O*-GlcNAcase action within COS-7 cells. By monitoring the level of *O*-GlcNAc-modified proteins using Western blot analysis, we found a clear time-dependent increase in levels of *O*-GlcNAcylated proteins. Even after 1 h of exposure to inhibitor (**9c**), increases in *O*-GlcNAc levels were observed. The inhibitor appears to quickly enter into the cells where it immediately blocks *O*-GlcNAcase activity, resulting in a time-dependent accumulation of *O*-GlcNAc-modified proteins (Fig. 6). After an initial rapid rise, the level of *O*-GlcNAcylated proteins in cells treated with inhibitor (**9c**) appears to approach symptotically a steady state within the cell (Fig. 6). This behavior is consistent with the similar time-dependent increase previously observed for HT29 cells incubated with PUGNAc (49). Western blot analysis of blots probed with anti-β-actin (Fig. 5*B*), followed by the appropriate secondary HRP-conjugate, revealed that in all cases the sample loading was equivalent. Also worth noting is that the parent compound NAG-thiazoline (**9a**) has been demonstrated previously to enter into cells where it exerts an effect on lysosomal β-hexosaminidase (65).

Conclusions—In summary, we show that human *O*-GlcNAcase and, by extension, members of family 84 of glycoside hydrolases are retaining glycosidases and use a mechanism involving substrate-assisted catalysis from the 2-acetamido group of the substrate. In this regard, the functionally

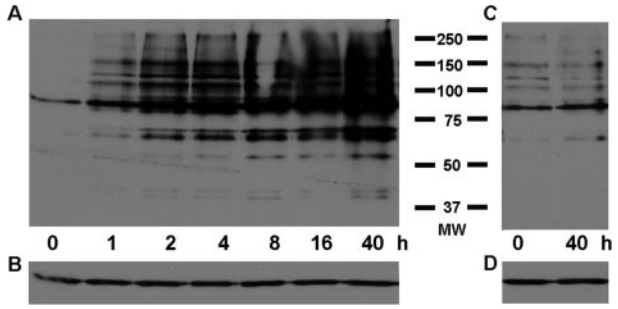

FIG. 6. **Incubation of COS-7 cells with thiazoline inhibitor (9c) results in a time-dependent increase in cellular levels of *O*-GlcNAc-modified proteins.** Western blot analyses of proteins from COS-7 cells cultured over 40 h in the presence or absence of 50 μM thiazoline inhibitor (**9c**). *A*, Western blot analysis of cellular *O*-GlcNAc levels as a function of time after exposure to inhibitor (**9c**) using anti-*O*-GlcNAc mAb CTD 110.6 followed by an anti-mouse IgG-HRP conjugate. *B*, Western blot of samples loaded in *A* treated with anti-β-actin mAb clone AC-40 followed by an anti-mouse IgG-HRP conjugate reveals equivalent β-actin levels in each sample. *C*, Western blot analysis of cellular *O*-GlcNAc levels as a function of time in the absence of inhibitor indicate that *O*-GlcNAc levels do not significantly change as a function of confluence. At 0-h plates were ≈25% confluent, and after 40 h plates were ≈90% confluent. *D*, Western blot of samples loaded in *C* treated as for *B* reveals equivalent β-actin levels in both samples.

related human enzymes *O*-GlcNAcase and lysosomal β-hexosaminidase, which both act to cleave terminal *N*-acetylglucosamine from glycoconjugates, use similar catalytic mechanisms despite their lack of sequence similarity. *O*-GlcNAcase, however, has an active site pocket that more readily tolerates moderately bulky substituents pendent to the acetamido group of the substrate than does the pocket of lysosomal β-hexosaminidase. Despite the similarity of the catalytic mechanism of these enzymes, we have exploited the differences in active site architectures between them to generate a small panel of potent inhibitors, some of which are remarkably selective for nucleocytoplasmic *O*-GlcNAcase over lysosomal β-hexosaminidase. Furthermore, these compounds are shown to function in cell culture where they result in dramatic increases in cellular *O*-GlcNAc levels. We anticipate that these inhibitors will be powerful tools in accurately dissecting the role of *O*-GlcNAc in model organisms and tissues without the generation of complex phenotypes stemming from concomitant inhibition of functionally related proteins.

Acknowledgments—We thank J. Hanover for the expression plasmid encoding *O*-GlcNAcase. We also thank T. Kitos and R. Cornell for assistance and access to tissue culture facilities and N. Cetinbas for technical assistance.

REFERENCES

1. Henrissat, B., and Bairoch, A. (1996) *Biochem. J.* **316,** 695–696
2. Henrissat, B., and Bairoch, A. (1993) *Biochem. J.* **293,** 781–788
3. Torres, C. R., and Hart, G. W. (1984) *J. Biol. Chem.* **259,** 3308–3317
4. Wells, L., Vosseller, K., and Hart, G. W. (2001) *Science* **291,** 2376–2378
5. Hanover, J. A. (2001) *FASEB J.* **15,** 1865–1876
6. Jackson, S. P., and Tjian, R. (1988) *Cell* **55,** 125–133
7. Kelly, W. G., Dahmus, M. E., and Hart, G. W. (1993) *J. Biol. Chem.* **268,** 10416–10424
8. Roos, M. D., Su, K., Baker, J. R., and Kudlow, J. E. (1997) *Mol. Cell. Biol.* **17,** 6472–6480
9. Lamarre-Vincent, N., and Hsieh-Wilson, L. C. (2003) *J. Am. Chem. Soc.* **125,** 6612–6613
10. Zhang, F., Su, K., Yang, X., Bowe, D. B., Paterson, A. J., and Kudlow, J. E. (2003) *Cell* **115,** 715–725
11. Vosseller, K., Wells, L., Lane, M. D., and Hart, G. W. (2002) *Proc. Natl. Acad. Sci. U. S. A.* **99,** 5313–5318
12. Lubas, W. A., Smith, M., Starr, C. M., and Hanover, J. A. (1995) *Biochemistry* **34,** 1686–1694
13. Griffith, L. S., and Schmitz, B. (1995) *Biochem. Biophys. Res. Commun.* **213,** 424–431
14. Cole, R. N., and Hart, G. W. (1999) *J. Neurochem.* **73,** 418–428
15. McClain, D. A., Lubas, W. A., Cooksey, R. C., Hazel, M., Parker, G. J., Love, D. C., and Hanover, J. A. (2002) *Proc. Natl. Acad. Sci. U. S. A.* **99,** 10695–10699
16. Yao, P. J., and Coleman, P. D. (1998) *J. Neurosci.* **18,** 2399–2411
17. Liu, F., Iqbal, K., Grundke-Iqbal, I., Hart, G. W., and Gong, C. X. (2004) *Proc. Natl. Acad. Sci. U. S. A.* **101,** 10804–10809
18. Chou, T. Y., and Hart, G. W. (2001) *Adv. Exp. Med. Biol.* **491,** 413–418
19. Braidman, I., Carroll, M., Dance, N., and Robinson, D. (1974) *Biochem. J.* **143,** 295–301
20. Ueno, R., and Yuan, C. S. (1991) *Biochim. Biophys. Acta* **1074,** 79–84
21. Dong, D. L., and Hart, G. W. (1994) *J. Biol. Chem.* **269,** 19321–19330
22. Toleman, C., Paterson, A. J., Whisenhunt, T. R., and Kudlow, J. E. (2004) *J. Biol. Chem.* **279,** 53665–53673
23. Gao, Y., Wells, L., Comer, F. I., Parker, G. J., and Hart, G. W. (2001) *J. Biol. Chem.* **276,** 9838–9845
24. Wells, L., Gao, Y., Mahoney, J. A., Vosseller, K., Chen, C., Rosen, A., and Hart, G. W. (2002) *J. Biol. Chem.* **277,** 1755–1761
25. Triggs-Raine, B., Mahuran, D. J., and Gravel, R. A. (2001) *Adv. Genet.* **44,** 199–224
26. Zhou, D., Mattner, J., Cantu Iii, C., Schrantz, N., Yin, N., Gao, Y., Sagiv, Y., Hudspeth, K., Wu, Y., Yamashita, T., Teneberg, S., Wang, D., Proia, R., Levery, S. B., Savage, P. B., Teyton, L., and Bendelac, A. (2004) *Science* **306,** 1786–1789
27. Legler, G., Lullau, E., Kappes, E., and Kastenholz, F. (1991) *Biochim. Biophys. Acta* **1080,** 89–95
28. Horsch, M., Hoesch, L., Vasella, A., and Rast, D. M. (1991) *Eur. J. Biochem.* **197,** 815–818
29. Liu, J., Shikhman, A. R., Lotz, M. K., and Wong, C. H. (2001) *Chem. Biol.* **8,** 701–711
30. Knapp, S., Vocadlo, D. J., Gao, Z. N., Kirk, B., Lou, J. P., and Withers, S. G. (1996) *J. Am. Chem. Soc.* **118,** 6804–6805
31. Lillelund, V. H., Jensen, H. H., Liang, X., and Bols, M. (2002) *Chem. Rev.* **102,** 515–553
32. Konrad, R. J., Mikolaenko, I., Tolar, J. F., Liu, K., and Kudlow, J. E. (2001) *Biochem. J.* **356,** 31–41
33. Liu, K., Paterson, A. J., Zhang, F., McAndrew, J., Fukuchi, K., Wyss, J. M., Peng, L., Hu, Y., and Kudlow, J. E. (2004) *J. Neurochem.* **89,** 1044–1055
34. Parker, G., Taylor, R., Jones, D., and McClain, D. (2004) *J. Biol. Chem.* **279,** 20636–20642
35. Arias, E. B., Kim, J., and Cartee, G. D. (2004) *Diabetes* **53,** 921–930
36. Junod, A., Lambert, A. E., Orci, L., Pictet, R., Gonet, A. E., and Renold, A. E. (1967) *Proc. Soc. Exp. Biol. Med.* **126,** 201–205
37. Bennett, R. A., and Pegg, A. E. (1981) *Cancer Res.* **41,** 2786–2790
38. Kroncke, K. D., Fehsel, K., Sommer, A., Rodriguez, M. L., and Kolb-Bachofen, V. (1995) *Biol. Chem. Hoppe-Seyler* **376,** 179–185
39. Yamamoto, H., Uchigata, Y., and Okamoto, H. (1981) *Nature* **294,** 284–286
40. Yamada, K., Nonaka, K., Hanafusa, T., Miyazaki, A., Toyoshima, H., and Tarui, S. (1982) *Diabetes* **31,** 749–753
41. Burkart, V., Wang, Z. Q., Radons, J., Heller, B., Herceg, Z., Stingl, L., Wagner, E. F., and Kolb, H. (1999) *Nat. Med.* **5,** 314–319
42. Roos, M. D., Xie, W., Su, K., Clark, J. A., Yang, X., Chin, E., Paterson, A. J., and Kudlow, J. E. (1998) *Proc. Assoc. Am. Physicians* **110,** 422–432
43. Gao, Y., Parker, G. J., and Hart, G. W. (2000) *Arch. Biochem. Biophys.* **383,** 296–302
44. Okuyama, R., and Yachi, M. (2001) *Biochem. Biophys. Res. Commun.* **287,** 366–371
45. Zachara, N. E., O'Donnell, N., Cheung, W. D., Mercer, J. J., Marth, J. D., and Hart, G. W. (2004) *J. Biol. Chem.* **279,** 30133–30142
46. Hanover, J. A., Lai, Z., Lee, G., Lubas, W. A., and Sato, S. M. (1999) *Arch. Biochem. Biophys.* **362,** 38–45
47. Liu, K., Paterson, A. J., Konrad, R. J., Parlow, A. F., Jimi, S., Roh, M., Chin, E., Jr., and Kudlow, J. E. (2002) *Mol. Cell. Endocrinol.* **194,** 135–146
48. Miller, D. J., Gong, X., and Shur, B. D. (1993) *Development* (*Camb.*) **118,** 1279–1289
49. Haltiwanger, R. S., Grove, K., and Philipsberg, G. A. (1998) *J. Biol. Chem.* **273,** 3611–3617
50. Mark, B. L., Mahuran, D. J., Cherney, M. M., Zhao, D., Knapp, S., and James, M. N. (2003) *J. Mol. Biol.* **327,** 1093–1109
51. Roeser, K. R., and Legler, G. (1981) *Biochim. Biophys. Acta* **657,** 321–333
52. Bergmann, M., and Zervas, L. (1931) *Ber. Dtsch. Chem. Ges.* **64,** 975–980
53. Kuroki, R., Weaver, L. H., and Matthews, B. L. (1999) *Proc. Natl. Acad. Sci. U. S. A.* **96,** 8949–8954
54. Zechel, D. L., and Withers, S. G. (2000) *Acc. Chem. Res.* **33,** 11–18
55. Vocadlo, D. J., Mayer, C., He, S., and Withers, S. G. (2000) *Biochemistry* **39,** 117–126
56. Vocadlo, D. J., Davies, G. J., Laine, R., and Withers, S. G. (2001) *Nature* **412,** 835–838
57. Mark, B. L., Vocadlo, D. J., Knapp, S., Triggs-Raine, B. L., Withers, S. G., and James, M. N. (2001) *J. Biol. Chem.* **276,** 10330–10337
58. Tews, I., Perrakis, A., Oppenheim, A., Dauter, Z., Wilson, K. S., and Vorgias, C. E. (1996) *Nat. Struct. Biol.* **3,** 638–648
59. Maier, T., Strater, N., Schuette, C. G., Klingenstein, R., Sandhoff, K., and Saenger, W. (2003) *J. Mol. Biol.* **328,** 669–681
60. Jones, C. S., and Kosman, D. J. (1980) *J. Biol. Chem.* **255,** 11861–11869
61. Terwisscha van Scheltinga, A. C., Armand, S., Kalk, K. H., Isogai, A., Henrissat, B., and Dijkstra, B. W. (1995) *Biochemistry* **34,** 15619–15623
62. Markovic-Housley, Z., Miglierini, G., Soldatova, L., Rizkallah, P. J., Muller, U., and Schirmer, T. (2000) *Struct. Fold Des.* **8,** 1025–1035
63. Mark, B. L., and James, M. N. G. (2002) *Can. J. Chem.* **80,** 1064–1074
64. Comer, F. I., Vosseller, K., Wells, L., Accavitti, M. A., and Hart, G. W. (2001) *Anal. Biochem.* **293,** 169–177
65. Tropak, M. B., Reid, S. P., Guiral, M., Withers, S. G., and Mahuran, D. (2004) *J. Biol. Chem.* **279,** 13478–13487
66. Hansch, C., and Leo, A. (1979) *Substituent Constants for Correlation Analysis in Chemistry and Biology*, pp. 1–339, John Wiley & Sons, Inc., New York

O-GlcNAcase Uses Substrate-assisted Catalysis: KINETIC ANALYSIS AND DEVELOPMENT OF HIGHLY SELECTIVE MECHANISM-INSPIRED INHIBITORS

Matthew S. Macauley, Garrett E. Whitworth, Aleksandra W. Debowski, Danielle Chin and David J. Vocadlo

J. Biol. Chem. 2005, 280:25313-25322.
doi: 10.1074/jbc.M413819200 originally published online March 28, 2005
